Int.J.HIT.TRANSC:ECCN.Vol.13: Special Issue NSEFCCIC (2026) Page 32-37 ISSN: 0973-6875

Available Online at www.hithaldia.in/locate/ECCN

ORIGINAL CONTRIBUTION

DESIGN, SIMULATION AND FABRICATION OF DUAL-BAND MICROSTRIP PATCH ANTENNA

[1]Dipan Das, [2]Surajit Mukherjee

[1]UG Student, Department of ECE, Haldia Institute of Technology, Haldia, West Bengal
[2]Assistant Professor, Department of ECE, Haldia Institute of Technology, West Bengal, India

ABSTRACT

This paper presents the design, simulation, and prototype realization of a compact dual-band microstrip patch antenna intended for wireless applications. A dual-band dual-mode structure that resonates at 2.7 GHz and 5.3 GHz is obtained by inserting two parallel I-shaped slots into the radiating patch. The slots create the second resonance while preserving a simple, low-profile geometry. The antenna is first dimensioned with the standard microstrip design equations and then refined through parametric sweeps in HFSS/CST on a 1.2 mm thick Arlon substrate (ε_r = 2.2). The optimized design yields return losses of –21.38 dB at 2.7 GHz and –23.04 dB at 5.3 GHz, together with broadside gains of approximately 7.33 dB and 7.38 dB, respectively. Radiation-pattern analysis shows predominantly broadside radiation at the lower frequency and additional lobes at 5.3 GHz arising from higher-order modes. A physical prototype is fabricated by PCB etching, fitted with an SMA connector, and measured. The measured results confirm the simulated performance, demonstrating that the antenna is well suited to compact dual-band use in WLAN, LTE and related wireless systems.

KEYWORDS: Dual-Band Antenna; Microstrip Patch Antenna; I-Shaped Slots; HFSS/CST; WLAN and LTE.

1. INTRODUCTION

The rapid expansion of wireless communication systems continues to drive demand for compact, lightweight, low-cost and efficient antennas capable of dual-band operation. Microstrip patch antennas remain attractive because of their planar geometry, low profile, straightforward fabrication and ease of integration with microwave circuits. Conventional single-patch designs, however, typically offer only a single resonance and limited bandwidth, gain and efficiency. Techniques such as slot loading, stacked patches, parasitic elements and defected ground structures have been widely explored to overcome these limitations. Among them, slot loading is particularly effective for dual-band operation: it perturbs the surface-current distribution and lengthens the effective current path without a significant increase in overall size.

In the present work a compact dual-band microstrip patch antenna for wireless applications is designed, simulated and fabricated. The design begins with the classical microstrip equations, after which two parallel I-shaped slots are introduced, and the geometry is optimized by full-wave parametric simulation. Reflection coefficient, VSWR, bandwidth, gain, efficiency and radiation patterns are evaluated. A prototype is then fabricated by standard PCB techniques and measured with a network analyzer. Agreement between measured and simulated data validates the approach.

2. ANTENNA DESIGN AND GEOMETRY:

The antenna is designed to operate at 2.7 GHz and 5.3 GHz on an Arlon substrate of relative permittivity ε_r = 2.2 and thickness 1.2 mm. The design flow comprises theoretical calculation of the initial patch dimensions, electromagnetic modelling, parametric optimization, fabrication and experimental verification. Standard rectangular-patch equations are first applied at the lower design frequency of 2.7 GHz. Two parallel I-shaped slots are subsequently etched on the

*Corresponding Address: ece.surajit@yahoo.com DOI 10.5281/zenodo.22038093

radiating patch; these slots alter the surface-current paths and introduce an additional resonance at 5.3 GHz while keeping the structure compact and simple.

The complete antenna comprises a rectangular radiating patch, two parallel I-shaped slots, the dielectric substrate, a ground plane and a microstrip feed line. Initial dimensions are refined by repeated full-wave simulations. The principal design equations are given below.

The Patch Width (w_p) is given by:

$$w_p = \frac{c}{2f_0}\sqrt{\frac{2}{\varepsilon_r + 1}}$$

The Effective Dielectric Constant (ε_{eff}) considering fringing effects is:

$$\varepsilon_{eff} = \frac{\varepsilon_r + 1}{2} + \frac{\varepsilon_r - 1}{2}\left(1 + \frac{12h}{w_p}\right)^{-1/2}$$

The Effective Patch Length is calculated as:

$$L_{eff} = \frac{c}{2f_0\sqrt{\varepsilon_{eff}}}$$

The Fringing Length Extension is:

$$\Delta L = 0.412h\frac{(\varepsilon_{eff}+0.3)(\frac{w_p}{h}+0.264)}{(\varepsilon_{eff}+0.258)(\frac{w_p}{h}+0.8)}$$

Finally, the Actual Patch Length is:

$l_p = L_{eff} - 2\Delta L$

Table 1: Final Optimised Antenna Dimensions

Parameter	**Dimension**
patch width (w_p)	39.501 mm
patch length (l_p)	33.009 mm
substrate width(w_s)	89.501 mm
substrate length (l_s)	83.36 mm
feed position (y_0)	12.881 mm
notch width	4.971 mm
feed-line width	2.42 mm
slot width	3 mm
slot length	17 mm
substrate height	1.2 mm

Arlon is chosen for its ready availability, moderate cost and suitability for laboratory fabrication; the 1.2 mm thickness provides a practical compromise between compactness and radiation efficiency. Copper is used for both the patch and the ground plane. Microstrip-line feeding is selected for its planar simplicity and compatibility with printed-circuit processes. The feed position is adjusted until S_{11} remains below –10 dB at both resonances. During optimization, patch size, slot geometry, feed location, substrate outline and ground-plane dimensions are varied systematically to improve return loss, impedance match, bandwidth, gain and pattern stability. The final geometry is realized as a three-dimensional electromagnetic model that incorporates accurate material parameters, finite conductor thickness, precise slot placement and a realistic feed transition before fabrication proceeds.

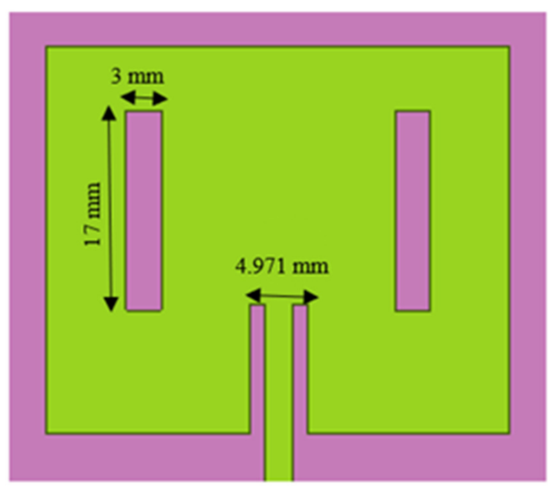

Figure 1: Slot and notch position on the patch

Figure 1 shows the slot and notch locations on the radiating patch.

The structure is enclosed in a radiation box with approximately quarter-wavelength clearance on all sides. Adaptive meshing is concentrated along the slot edges, the feed gap and the patch perimeter. Two frequency sweeps are employed: a discrete sweep for gain and radiation patterns at the two design frequencies, and an interpolating sweep from 2 GHz to 8 GHz to obtain the broadband return-loss response.

3. WORKING PRINCIPLE:

The generation of higher and lower resonant frequencies in a slotted patch antenna mainly depends on the current path length and the resonance characteristics of the patch.

3.1 Lower-Frequency Generation:

The slots produce a discontinuity in the direct path of the surface current. Consequently, the current is forced to flow around the slot, which increases the effective electrical length of the patch. Since the longer current path produces a lower resonant frequency. Thus, the I-shaped slots help generate the lower-frequency resonance. Figure 2 presents the top view of the dual-band antenna, illustrating the current paths associated with the lower resonance.

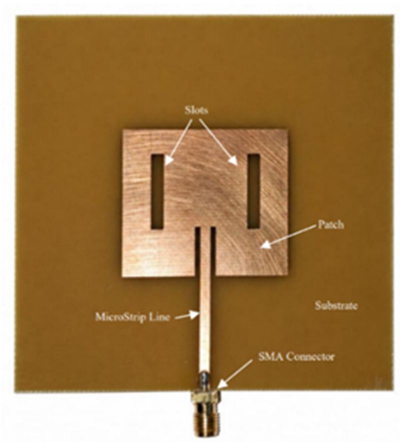

Figure 2: Top view of the “Dual-Band” microstrip patch antenna

3.2 Higher-Frequency Generation:

The portion of the patch that lies outside the slots supports a shorter current path and therefore resonates at the higher frequency of 5.3 GHz. Edge modifications and the slot geometry also excite higher-order modes that contribute to the upper band. Figure 3 shows the corresponding back view of the antenna.

Figure 3: Back view of the “Dual-Band” microstrip patch antenna

3.3 Dual-Band Operation:

The two current paths therefore establish the two operating frequencies: the longer path around the slots yields 2.7 GHz while the shorter residual path yields 5.3 GHz. Proper choice of slot dimensions and feed location enables simultaneous good matching at both frequencies.

4. FABRICATION:

Once simulation results are judged satisfactory, the layout is transferred to a 1.2 mm Arlon substrate with copper cladding on both sides. The pattern is defined by toner-transfer etching, producing the dual-slot patch and microstrip feed. An SMA connector is soldered to the feed line to complete the prototype. Figure 4 shows the isometric view of the simulated antenna.

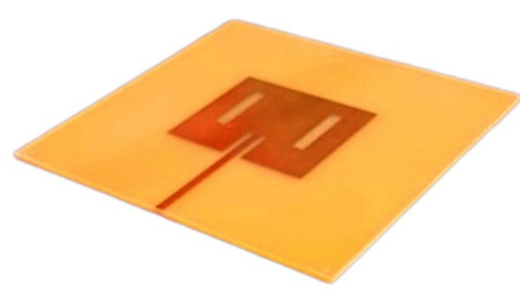

Figure 4: Isometric view of the “Dual-Band” microstrip patch antenna

The pattern is etched using toner transfer methodology following application on Arlon to obtain the required microstrip line with dual slots and fed with an SMA connector in the input feed line, as the desired prototype of the antenna is fabricated in its ready form as displayed in Figure 2 and 3. Photos are given for the Top view of the fabricated antenna, including the dual slots and patch and their feeding line, and for its bottom view displaying a solid ground plane. The slots and feeding line align within the specified limits from their simulated values.

5. RESULT:

The proposed dual-band microstrip patch antenna was designed and analysed using full-wave electromagnetic simulation software (HFSS/CST) for operation at 2.7 GHz and 5.3 GHz. Two parallel rectangular slots were incorporated into the radiating patch to generate dual-band characteristics and increase the effective current path length.

5.1 Return Loss (S_{11}):

The simulated results show two distinct resonances with good impedance matching. At 2.7 GHz, the return loss is approximately −21.38 dB, while at 5.3 GHz, it is approximately −23.04 dB. Both values are below the −10 dB reference level, confirming satisfactory impedance matching and dual-band operation. Figure 5 displays the simulated return-loss curve over 2–8 GHz.

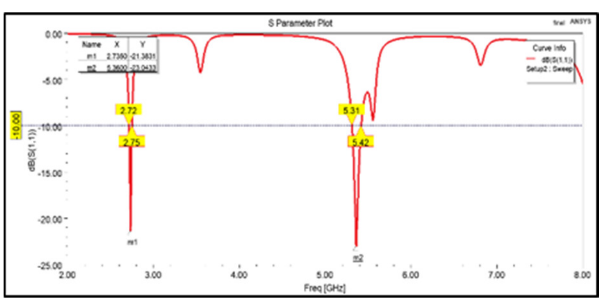

Figure 5: Return Loss (S_{11}) Plot of the Antenna

5.2 Peak Realized Gain:

The antenna provides stable gain at both resonant frequencies. The peak realized gain is approximately 7.33 dB at 2.7 GHz and 7.38 dB at 5.3 GHz, indicating satisfactory radiation performance and effective power transfer. Figure 6 shows the peak-gain response versus frequency.

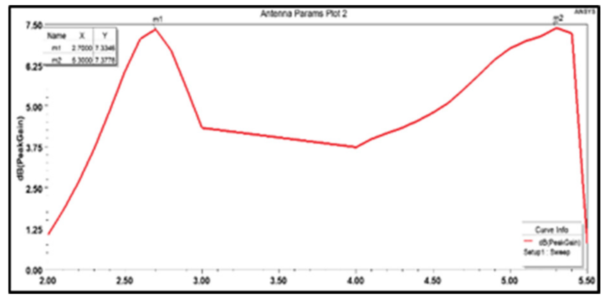

Figure 6: Peak Gain Plot of the Patch Antenna

5.3 Radiation Pattern at 2.7 GHz:

The φ = 0° and φ = 90° planes exhibit broadside radiation with stable gain and effective current concentration around the patch edges and slot regions, confirming efficient resonance at 2.7 GHz. Figures 7 and 8 present the E-plane and H-plane patterns at 2.7 GHz, respectively.

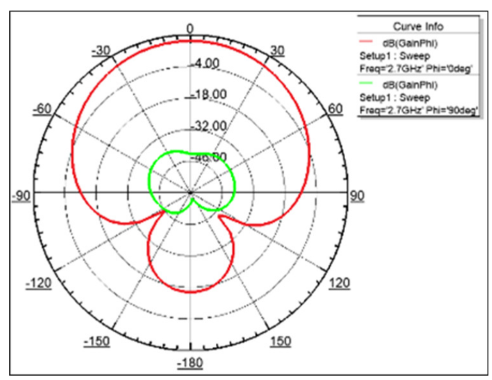

Figure 7: Radiation Pattern at 2.7 GHz (E-Plane)

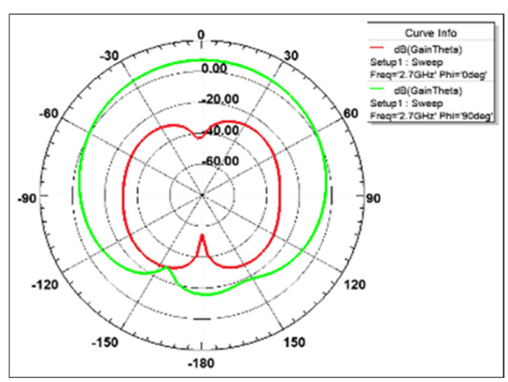

Figure 8: Radiation Pattern at 2.7 GHz (H-Plane)

5.4 Radiation Pattern at 5.3 GHz:

At the higher frequency, additional lobes are observed due to higher-order resonant modes associated with the slot structure. Slight asymmetry in the φ = 0° and φ = 90° planes, along with more noticeable back lobes and nulls, is observed due to surface-current redistribution and scattering effects. Figures 9 and 10 show the corresponding E-plane and H-plane patterns at 5.3 GHz.

5.5 Overall Performance:

The proposed antenna successfully achieves dual-frequency operation at 2.7 GHz and 5.3 GHz with low return loss, stable gain, and acceptable radiation characteristics. The parallel slot configuration provides dual resonance while maintaining a compact, low-profile, simple, and cost-effective structure.

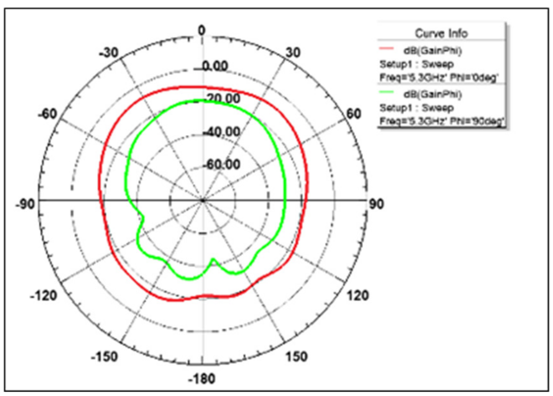

Figure 9: Radiation Pattern at 5.3 GHz (E-Plane)

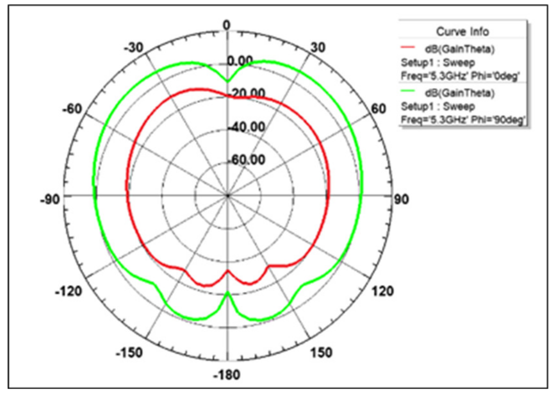

Figure 10: Radiation Pattern at 5.3 GHz (H-Plane)

6. CONCLUSION

A compact dual-band microstrip patch antenna array containing two parallel rectangular slot-etched elements for operation at 2.7 GHz and 5.3 GHz was designed, simulated and developed. Design specifications obtained, such as the return loss being below 19 dB, the gain being approximately 7.3 dB, and broadside radiation being observed mostly, are in accordance with the obtained values from manufactured results to accommodate a specific range of applications like WLAN and LTE.

REFERENCES

[1] C. A. Balanis, (2016). Antenna Theory: Analysis and Design. 4th ed., John Wiley & Sons.

[2] R. Garg, P. Bhartia, I. Bahl and A. Ittipiboon, (2001). Microstrip Antenna Design Handbook. Artech House, 2001.

[3] D. M. Pozar, (1992). Microstrip Antennas. *Proceedings of the IEEE*, 80(1), 79–91.

[4] Y. X. Guo, K. M. Luk and K. F. Lee, (2002). Dual-Band Slot-Loaded Microstrip Patch Antenna. *IEEE Transactions on Antennas and Propagation*, 50(1), 65–67.

[5] K. L. Wong, (2002). Compact and Broadband Microstrip Antennas. John Wiley & Sons.

[6] N. Behdad and K. Sarabandi, (2010). A Multiresonant Single-Element Wideband Slot Antenna. *IEEE Transactions on Antennas and Propagation*, 58(5), 1740–1743.

[7] J. Anguera, C. Puente, C. Borja and J. Soler, (2003). Dual-Frequency Broadband Stacked Microstrip Antenna. *IEEE Antennas and Propagation Magazine*, 45(2), 10–22.

[8] S. Maci and G. B. Gentili, (1997). Dual-Frequency Patch Antennas. *IEEE Antennas and Propagation Magazine*, 39(6), 13–20.

[9] W. C. Liu, C. M. Wu and N. C. Chu, (2010). A Compact CPW-Fed Slotted Patch Antenna for Dual-Band Operation. *IEEE Antennas and Wireless Propagation Letters*, 9, 110–113.

[10] K. F. Tong and T. P. Wong, (2007). Circularly Polarized U-Slot Rectangular Patch Antenna. *IEEE Transactions on Antennas and Propagation*, 55(8), 2382–2385.